POP - ANALYSIS OF GLOBAL LARGE-SCALE TRAVELLING ROSSBY WAVES

REINER SCHNUR AND HANS VON STORCH

Max-Planck-Institut für Meteorologie
Hamburg, Federal Republic of Germany

A global investigation of zonally propagating large-scale Rossby waves in observed data has been performed using the method of Principal Oscillation Pattern (POP-) Analysis which is a technique for identifying time-dependent patterns in multivariate time series.

The analyzed data consist of twice-daily fields of 500 mb geopotential heights from 1984-87 ECMWF analyses. All time variations on time scales below 3 and above 25 days were first removed. Then the zonal wave number 1-9 Fourier coefficients were examined with POP Analysis separately for the three winters (DJF) 84/85 to 86/87 and for the summers (JJA) 85 to 87.

For each of the zonal wave numbers 1 to 4 the dominant modes detected in both seasons are waves that are symmetric about the equator and travel westward in the tropical belt 40°S - 40°N with a period of about 7 days. For the higher wave numbers 5 to 9 the POP-Analysis reveals eastward propagating wave patterns in both the southern and the northern hemisphere. Most periods are in the range of 4 to 6 days. There is no evidence for the existence of globally coherent waves with significant amplitudes on both hemispheres in this case. An analysis of the vertical structure of the modes by means of associated correlation patterns shows that all waves are barotropic external Rossby waves.

A comparison of the results with the findings of a conventional wavenumber-frequency analysis shows that the POP-Analysis is an easy-to-use and convenient method for isolating oscillatory patterns in geophysical data without making a-priori assumptions about the relation between standing and travelling components of the field.

1. INTRODUCTION.

The linear solution of the problem of free waves in an isothermal atmosphere on a rotating sphere goes back until Laplace's theory of tides (1799 to 1823) and involves separation of the linearized primitive equations into their horizontal and vertical dependencies. Solving the horizontal structure equations (Laplace's tidal equations) through a zonal wavenumber/frequency - ansatz two classes of solutions are obtained: solutions of the "first class" (gravity waves) and solutions of the "second class".

The latter waves result from rotation of the earth and the spherical geometry. They represent the resonant state of the atmosphere (normal modes) and are called **Rossby waves**. Their latitudinal structure for the geopotential height fields is given by the so-called **Hough** functions $\mathbf{H}_{\mathbf{n}}^{\mathbf{m}}$ for a 10-km equivalent depth of the atmosphere (Longuett-Higgins, 1968). Here m is the zonal wave number and n-m is the number of nodal points in the streamfunction profile between the north and the south poles. The vertical structure equations yield external Rossby waves, with geopotential and velocity amplitudes which grow exponentially with height ('Lamb waves').

Rossby et al. (1939) proposed that much of the characteristics of the atmospheric flow can be captured by only regarding it's rotational part. When they calculated one-dimensional plane wave solutions of the vorticity equation in a non-divergent barotropic atmosphere with infinite lateral boundaries they found the dispersion formula

$$c = U - \beta L_x^2 / 4\pi^2 \qquad (1)$$

where c is the zonal phase speed, U is some constant zonal current, β is the change df/dy of the Coriolis parameter $f = 2\Omega\sin\phi$ at a latitude ϕ, Ω is the angular speed of rotation and L_x is the zonal wavelength.

Equation (1) is used later to compare the phase speeds of the POPs with the theoretically expected values. For so-called **ultralong** or **planetary-scale** waves (wave numbers 1 to 4) typical phase speeds would be 227 m/s westward to 5 m/s eastward, as derived from (1) at 50° S and for a westerly zonal current of 20 m/s. The corresponding periods are 1.3 days westward to 14.9 days eastward. For **long** or **large-scale** waves (wave numbers 5 to 9) the phase speeds and periods are 5 to 17 m/s, resp. 6 to 2 days eastward. Obviously, these values can serve only as rough estimates for real phase

speeds and periods. E.g. inclusion of divergence effects or lateral boundaries can modify the phase speeds considerably, especially for lower wave numbers.

There have been some studies in the past attempting to find evidence for the existence of normal mode Rossby waves in the real atmosphere. Apart from being interesting for the understanding of the general circulation knowledge of these ultralong and long travelling waves is also important as a diagnostic tool for the interpretation of general circulation model results. Extensive reviews on planetary-scale Rossby waves have been published e.g. by Madden (1979) and Salby (1984). A comparison of the appearance of planetary-scale travelling waves in observational data from ECMWF analyses and data from a general circulation model using wavenumber-frequency analysis can be found in Barbulescu (1990).

In this paper the method of Principal Oscillation Pattern Analysis is used to find observational evidence for the existence of ultralong and long travelling Rossby waves in the real atmosphere. In doing so the analysis method itself can be tested by comparing the findings with results from other techniques. On the other hand the study should clarify the horizontal and vertical structure of the Rossby waves, especially the questions are addressed whether the detected modes are global features of the atmosphere and if they can be identified with the theoretically expected Hough functions. In this context, it is emphasized that the POP Analysis yields spatial patterns without making any a priori assumption about the meridional structure of the modes. This is in contrast to some other methods which use predetermined basis functions like spherical harmonics or Hough functions. The POP method is described in the next section together with the data used and the analysis performed.

2. ANALYSIS AND DATA.

a) Principal Oscillation Patterns and Associated Correlation Patterns.

Principal Oscillation Pattern (POP-) Analysis (Hasselmann, 1988; Storch et al., 1988; Storch et al., 1990) is a technique for identifying time dependent regularly developing spatial patterns in multivariate time series whose dynamics are unknown or too complex. When using this method the basic assumption is that the evolution of a n-dimensional stochastic vector process $\mathbf{x}(t)$ can be written as a first-order linear Markov process

$$\mathbf{x}(t+1) = \mathbf{A} \cdot \mathbf{x}(t) + \text{noise} \qquad (2)$$

where the system matrix $\mathbf{A}$ is estimated from the data as the normalized lag-1 autocovariance matrix of $\mathbf{x}(t)$.

In most cases, the system (2) (with zero noise) has a complete set of linearly independent eigenmodes. The complex eigenvectors $\mathbf{P}_j = \mathbf{P}^1_j + i\,\mathbf{P}^2_j$ of $\mathbf{A}$ are called Principal Oscillation Patterns (POPs). Their projection onto the original data set, using

$$\mathbf{x}(t) = \sum_{j=1}^{n} z_j(t)\,\mathbf{P}_j \quad ,$$

yields the POP coefficient time series $z_j = z^1_j + i\,z^2_j$, each of which defines a damped harmonic oscillation with a period and e-folding time given through the corresponding (complex) eigenvalue. So the dynamical evolution of the system described by one POP $\mathbf{P}$ with period T can be visualized by the following infinite cyclic sequence:

$$\begin{array}{ccc} \mathbf{P}^2 & \xrightarrow{\quad T/4 \quad} & \mathbf{P}^1 \\ \uparrow T/4 & & T/4 \downarrow \\ -\mathbf{P}^1 & \xleftarrow{\quad T/4 \quad} & -\mathbf{P}^2 \end{array} \qquad (3)$$

Note that the POP patterns themselves are only defined to multiplication with an arbitrary complex factor. They are normalized so that they have a constant norm and so that the real and imaginary components are orthogonal. The magnitude of an oscillation is then given through the POP coefficient time series.

After having found a significant pair of POPs, $\mathbf{P}^1$ and $\mathbf{P}^2$, with POP

coefficients $z^1(t)$ and $z^2(t)$, it is often useful to know about the signal's appearance in other variables, say v(t). For that purpose associated correlation patterns, Q^1 and Q^2, can be derived as solution of

$$< \| v(t) - (z^1(t)/\sigma^1)\, Q^1 - (z^2(t)/\sigma^2)\, Q^2 \|^2 > = \text{Min} ,$$

where $\|.\|$ is a quadratic norm, <.> is expectation. The POP coefficients are divided by their standard deviations, σ^1 and σ^2, in order to obtain the associated patterns in the same units as the investigated variable v.

The oscillatory evolution of the system described in the POP cycle (4) is then reflected in the associated correlation pattern through the cycle

$$\ldots \longrightarrow Q^2 \longrightarrow Q^1 \longrightarrow -Q^2 \longrightarrow -Q^1 \longrightarrow Q^2 \longrightarrow \ldots .$$

b) Data and analysis.

The data set used in this study is taken from the ECMWF Global Analysis Data Set and consists of twice daily data for 1984 to 1987, on a 2.5 × 2.5 grid and for the seven levels 850, 700, 500, 300, 200, 100 hPa. In this time interval the analyses are fairly stationary (cf. Trenberth and Olson, 1988). The variable analyzed with the POP method is 500 hPa geopotential height. Associated correlation patterns were derived for all six levels.

The following points concerning the pre-processing of the data for the POP ananlysis are to be noticed:

- Since we are looking for signals with periods longer than two days and shorter than about four weeks all data were first band-pass filtered so that only time scales between 3 and 25 days were retained.
- There were separate POP analyses for eight data sets: The three northern winters (DJF) 84/85 to 86/87 and the three northern summers (JJA) 85 to 87 were extracted. For each season, four latitude bands were then extracted from the data, namely a global area from 85°S to 85°N (G), the northern hemisphere from 10°N to 85°N (NH), the southern hemisphere from 85°S to 10°S (SH) and the tropical region from 35°S to 35°N (TR).
- The data were Fourier decomposed along each latitude, using the standard scheme.The result was one vector time series for each wave number, with each vector consisting of the cosine and sine coefficients for all latitudes.
- These time series were expanded in Empirical Orthogonal Function (EOF) series in order to remove small-scale noise and to reduce the dimension of the system. The expansion was truncated after 18 EOFs, retaining more than 95 % of the total variance.

The time dependent EOF-coefficients (Principal Components) resulting from the above procedure were taken as input vector time series for the subsequent POP analyses. In order to account for the varying amplitude scales of the geopotential height for different latitude bands each POP analysis is performed for the original data and, additionally, for the normalized data where each value is divided by its (local) standard deviation.

Only those POPs are considered which satisfy the following criteria:

- The e-folding time is not less than one time step and the ratio of the e-folding time and the oscillation period is greater than 1/4 .
- The percentage of variance which the POP explains in the data is not too small, at least say 5 %.
- A cross-spectral analysis of the real and imaginary part of the POP coefficient time series shows
  - variance maxima
  - a relative phase of ±90°
  - a high squared coherence

  at or near the POP period.
- After transforming the POPs back into physical space the real and imaginary parts of the POP show a behavior which can be physically interpreted, e.g. as a travelling or standing wave (see below).

Clearly, these criteria allow for some subjective judgement.

There are basically three types of geometrical waveforms that can be defined by a POP of zonal Fourier coefficients. They are schematically drawn in Figure 1, also showing the two forms of representation which will be used. The sample POPs are given for the case that the variances of the real and imaginary components of the POP coefficient time series are nearly equal, as is the case for all POPs discussed in this paper.

If the real and imaginary parts are 90° out of phase (i.e. a quarter of a wavelength) and if the amplitudes are nearly equal the two patterns describe a purely zonally propagating wave according to the transformation cycle (4) (Fig. 1a). One has a standing wave if the amplitude of one component is very small compared to the other (Fig. 1b). The case of relevant amplitudes of significantly different magnitudes is possibly indicative for a superposition of a propagating wave with a standing component (not shown). A meridional shift between the amplitudes of the real and imaginary part of a POP (Fig. 1c) means that the oscillation

describes a meandering travelling wave.

Due to the notion of zonal Fourier decomposition for single wave numbers a natural limitation of the method used in this study is as follows. Since the wavelength for a specific zonal wave number is shorter in higher than in lower latitudes the zonal scale of POP patterns must decrease with increasing distance from the equator. Moreover, the Fourier coefficients describe global patterns around whole latitude circles. Thus, it is not possible to identify patterns with features of equal scale in different latitude bands or regional patterns as e.g. the Pacific / North America (PNA) pattern.

After having identified a Rossby wave with a certain POP, associated correlation patterns were derived in order to gain further insight into the horizontal structure and to examine the vertical structure of the wave. For each analysis, this was done for the geopotential height data of the levels 100, 200, 300, 500, 700, 850 hPa. Because in the tropics the divergent part of the flow is expected to play a role, associated correlation patterns were additionally derived in the TR-analyses for streamfunction and velocity potential fields, which were computed from the wind fields of the ECMWF data. Prior to the computation of the associated correlation patterns, the mean and the semiannual and the annual cycles were removed from the data, and only the zonal wave numbers 1 to 4 (for POPs of wave numbers 1 to 4), resp. the wave numbers 5 to 9 (for POPs of wave numbers 5 to 9) were kept.

3. RESULTS.

3.1. Zonal wave numbers 1 to 4.

Table 1 shows all significant POPs found in the zonal wave number domain 1 to 4 for the three winters (DJF) 84/85 to 86/87. The most prominent feature that can be seen is one POP in the tropical analysis (TR) for each of the four wave numbers. In addition, there is one POP in the wave-1 TR-analysis and one for wave number 2 in the northern hemisphere (NH). The first mode will be examined in detail in section a) while the rest of the patterns are briefly summarized in b). The results for the summer (JJA) analyses 85-87 are given in table 2 and are shortly discussed in c). The findings for the planetary scale waves are compared to those obtained from a wavenumber-frequency analysis in d).

a) One specific POP in northern winter.

The first wave number 1 POP shown in table 1 is a westward travelling wave in the tropical region explaining 23.4 % of the variance. Unless otherwise stated, this percentage always refers to the variance in the time and space filtered data, i.e. especially to the single zonal wave number under consideration. Figure 2 shows the real and imaginary part of the POP after reconstruction from EOF space into physical space. The plot of the relative phase in Fig. 2b exhibits a clear phase shift of 90°, i.e. one quarter of the wavelength. A cross spectral analysis of the real and imaginary part of the POP coefficient time series (Figure 3) also shows a phase shift of -90°, so that the POP describes a westward propagating wave according to the POP cycle (4).

The oscillation period is 7.6 days with an e-folding time of 6 days, i.e. almost one full oscillation length. The POP coefficients have a broad maximum of the variance spectrum near the period and their squared coherence at the period which is above the 99% significance level (Fig.3).

The POP has maximum amplitudes at about -25°S and at +25°N (real part), resp.+40°N (imaginary part). There is almost no phase shift with latitude so that this POP has a global structure symmetric about the equator and thus resembling the first symmetric normal mode. It could be the so-called

5-day wave (Madden,1979), which corresponds to the H_2^1 mode with maximum amplitude equatorwards of ±50°. The somewhat greater POP period, 7.6 instead of 5 days, is possibly an overestimation and, indeed, the cross spectra show maximum variance and coherence at the period of 5 days (Fig. 3).

The wave exhibits a meridional displacement of its amplitude maximum in the northern hemisphere between real and imaginary part (Fig.2b). The POP is thus a purely zonally propagating feature in the southern hemisphere whereas in the northern hemisphere the POP is a mixture of a zonally propagating and a standing component and, possibly, a meridionally propagating component. This systematic deviation from the zonal propagation might be due to the real wind conditions (nonzonal mean wind) or to topographic effects (Himalaya).

This first POP in the tropical region can also be identified in the global analysis (GL), but only in the normalized data because of smaller amplitudes in the tropics than in higher latitudes (not shown). Due to the normalization, this POP has no longer two maxima on both sides of the equator but only one maximum over the equator.

Figure 4a shows the associated correlation pattern of the POP for geopotential height in the 850 hPa level, after removal of the annual cycle and after truncation to the first four zonal waves. The pattern has roughly the same horizontal structure as the corresponding POP and explains up to 25% of the total variance.The associated correlation patterns for the other levels reveal the same structure with nearly constant phase in the vertical (Fig. 4b). The patterns also show an increasing amplitude below 200 hPa and decreasing amplitudes above 200 hPa (Fig. 4b). Thus, the first wave-1 POP has the vertical structure of a barotropic external Rossby wave. The decrease of the amplitude in the upper atmosphere has also been reported for the Rossby waves studied so far (e.g. Madden, 1979).

The same statements can be made for the associated correlation patterns for the stream function data although the explained variance in this case is very low. The associated patterns for the velocity potential are negligible in terms of the explained variances. Thus, this wave which has been found in the TR-analysis with maxima at ± 30° seems not to be connected to the divergent features of the tropical circulation.

b) Summary in northern winter (Table 1).

As already mentioned at the beginning of section 3.1 there is also one POP in the TR-analysis for each of the wave numbers 2, 3 and 4. They travel westwards with periods between 6 and 7.5 days, and they have a symmetric structure, similarly to the wave-1 POP discussed above, with maximum amplitudes at about ±35° (Fig. 5). However, the explained variances and also the coherencies of the real and imaginary coefficients are not as high as in the wave number 1 case. The wave-3 and wave-4 POPs again show a meridional displacement of their amplitude maxima in the northern hemisphere between real and imaginary part (Fig.5b,c).

There is one other POP in the TR-analysis for wave number 1, representing a westward propagating wave with a period of 19 days. It has maximum amplitudes at about 40°S and 40°N, but with an antisymmetric structure, and explains 25.6% of the wave-1 variance. The coherence of the real and imaginary part of the coefficient time series is not as high as in the first case.

The most conspicuous POP in table 1 is a wave for zonal wave number 2 in the northern hemisphere with an explained variance of 36.4 %. It has a maximum amplitude at 60° N, whereby the maximum of the real part is somewhat greater than that of the imaginary part (Fig. 6). This fact seems to be again indicative for the presence of a standing component in the pattern.

There are no other POPs in the GL-, SH- and NH-analyses to which the authors would attribute enough correspondence with the criteria of section 2.

In all cases, the associated correlation patterns confirm the character of the planetary scale modes as external Rossby waves, with almost no phase shift in the vertical and with increasing amplitudes below 200-300 hPa.

c) Summary in northern summer (Table 2).

The results for the northern summer (JJA) analyses are summarized in table 2. The four first symmetric modes in the TR-analysis, with westward propagation, were also identified for the summer season. The explained variances of all but the first and the coherencies of the coefficient time series are, however, lower than in the winter. Their structure shows a

slight meridional shift of amplitude maxima between real and imaginary part in the southern hemisphere, as it is the case on the opposite hemisphere for the POPs in the winter season.

In contrast to the winter case for each wave number there are additional POPs in the southern hemisphere with maxima at 45°S to 65°S. Only for wave number 1 they show westward, otherwise eastward propagation.

d) Comparison with a wavenumber-frequency analysis.

The results of the POP analyses presented so far for the planetary scale wave numbers can be compared to the results of a similar study which used the method of wavenumber-frequency analysis (Hayashi, 1977, 1982). Barbulescu (1990) calculated coherence and phase spectra between travelling waves in eight years of ECMWF analyses geopotential heights as well as in general circulation model data fields in order to isolate global large scale travelling waves.

He found symmetric modes for wave numbers 1 to 4 with periods of about 5, 4, 4.5 and 6 days, resp. Figure 7 shows as an example the spectrum of the wave-1 mode in the 300 hPa level. One can see a coherent wave structure which ranges from about 40° S to 40° N for the period of 5 days (Fig. 7a) in accordance with the POPs in the TR analyses in this study. The phase difference in Fig. 7b shows an in-phase structure in the region of ± 40° thus also indicating a global symmetric wave around the equator. In the other three cases a similar structure is detected with the exception of the phase difference for wave number 4. The coherencies for waves 1 and 2 are significantly greater than for waves 3 and 4 which means that these former waves were found less often than the latter. Remember that for wave number 3 and 4 the POPs found are not too pronounced as well.

Barbulescu also detected the same vertical structure of the normal modes as reported in the literature and in this section of the study, namely constant phase (or weak westward tilt) and amplitudes exponentially increasing from the bottom to about 200 hPa and decreasing in the upper atmosphere.

Similar to the POP analyses, Barbulescu found only little evidence for the existence of normal modes with higher meridional indices n-m. He can report only single events of the first antisymmetric and the second symmetric waves in selected winter and summer seasons.

3.2. Zonal wave numbers 5 to 9.

The results for the large-scale waves are listed in table 3 and 4. They differ from those shown in the previous section in that for each wave number one or two eastward migrating Rossby waves exist in both the southern and the northern hemisphere and no additional POPs in the TR-analysis were found. As an example, the first modes for wave number 6 in both hemispheres are discussed again in some detail in section a), followed by summaries for winter and summer.

a) Two specific POPs in northern winter.

The first POP in the southern hemisphere for wave number 6 explains 28% of the wave-6 variance and is plotted in Figure 8a. It shows a homogeneous oscillation pattern with an amplitude maximum at 50°S. The real and imaginary parts have equal amplitudes over the whole latitude band with a phase shift of 90° where the amplitudes are nonzero. The results of the cross spectral analysis of the POP coefficient time series (Fig. 8b) show features which are common to almost all POPs in this part of the study, namely pronounced variance maxima and extremely high coherencies at the POP period.

In the northern hemisphere, there is a wave-6 POP (Fig. 9) with a peak at 50°N and a similar horizontal structure. Its oscillation period is 6.3 days (eastward).

As is the case for most of the POPs in the wave number domain 1 to 4 there are also POPs in the GL-analysis which correspond to the above mentioned hemispheric waves. However, no global patterns are found which have significant amplitudes on both hemispheres, contradicting the notion of global waves. In order to further investigate whether the two oscillations which are given by the NH- and SH-POPs are related to each other, a complex cross spectral analysis (Gonella, 1972) between the complex coefficient time series of the SH- and NH-patterns was performed. If such a relationship existed, the phase spectrum would be constant and the coherence would be high, at least near the POP period. Since these conditions were not fulfilled it is concluded that the POPs in the two hemispheres are independent dynamical entities.

For the calculation of associated correlation patterns the wave numbers 5 to 9 were now retained in the geopotential height data at the different levels. The associated patterns for the above described SH- and NH-POPs (Figures 8 and 9), presented in Figure 10 for the level 850 hPa, have explained variances of up to 20% at latitudes with significant POP amplitudes. They reveal the same clear structure than the POPs themselves: the real and imaginary part are exactly out of phase and define a zonally propagating wave. The pattern in the northern hemisphere has greater wave amplitudes over the storm track areas over the Atlantic whereby the southern hemisphere pattern is more equally distributed. The analysis of the vertical structure of the modes is again consistent with external Rossby waves (not shown).

b) Summary in northern winter (Table 3).

As can be seen in table 3 the most dominant feature in the domain of the large-scale waves in both hemispheres is one wave for each wave number with an amplitude maximum at 50°S, resp. 40°-50°N, and with explained variances between 16% and 51%. The oscillation periods range from 3.5 to 6.3 days, with the exception of the wave number 5 POPs. These in general shorter periods (faster phase speeds) for smaller horizontal scales, as against the planetary-scale modes in section 3.1, are in accordance with the Rossby wave theory (cf. (1)).

The lower parts of tables 3a and 3b list additional POPs found in the two hemispheres. Except for two cases they have two amplitude maxima, with one being only secondary (as indicated).

As described in a), there are no coherent global patterns with significant amplitudes on both hemispheres. All waves have a vertical structure which is characteristic for external Rossby waves.

c) Summary in northern summer (table 4).

In northern summer the results for the wave numbers above 5 are again comparable to the winter case, with somewhat lower explained variances. In the northern hemisphere (local summer) there are less POPs than in the winter analysis, with smaller amplitudes, and the amplitude maxima of the patterns are partly shifted about 10° northwards. The amplitudes of the southern hemisphere POPs (local winter) are not significantly greater than

in the DJF case, although the associated correlation patterns reflect somewhat stronger signals.

4. SUMMARY AND DISCUSSION.

In this paper there have been presented the results of a series of POP analyses which were performed in order to isolate global ultralong (wave numbers 1 to 4) and long (wave numbers 5 to 9) Rossby waves in the geopotential height field. The data were time filtered to retain only time periods between 3 and 25 days and spatially Fourier decomposed along each latitude. Besides that the analyses assumed no a priori horizontal structure.

In northern winter (DJF), for each of the zonal wave numbers 1 to 4 one wave has been found resembling the first symmetric Hough mode. Especially the wave-1 mode is the well-known 5-day wave. For wave number 1 also one mode with an antisymmetric structure was found. These waves have amplitude maxima at about 30° on both sides of the equator. The wave-2 mode in the northern hemisphere has maximum amplitude at 60°N. For the higher wave numbers the analyses detected mostly two waves in both hemispheres with one, resp. two amplitude maxima at higher latitudes. In northern summer (JJA) the results are similar though partly less clear.

Apart from the symmetric waves for the four lowest wave numbers there is no evidence for the existence of global waves with significant components on both hemispheres. Clearly, an identification of the horizontal structure of the single-hemispheric patterns with symmetric or antisymmetric Hough functions is not unambiguously possible.

With the aid of the technique of associated correlation pattern analysis it could be shown that the vertical structure of the POPs is that of barotropic external Rossby waves, as expected from simplified theory of free normal modes in an isothermal atmosphere.

Waves 1 to 4 travel westwards, waves 5 to 9 travel eastwards in accordance with the dispersion formula. Table 5 shows the the phase speeds of the POP patterns as derived from the POP period and the theoretically expected values which were derived from the dispersion formula (1) after computation of the mean zonal wind from the ECMWF wind data. The phase speeds disagree for the lower wave numbers, but for higher wave numbers than 5 the agreement is fair in both hemispheres.

The results of this investigation have also been compared with that of a similar study which used conventional wavenumber-frequency analysis

(Barbulescu, 1990). This method has been generally come into use since the seventies to isolate oscillatory features in geophysical data. The easy-to-use POP analysis method has proved to be convenient as well for this kind of problem, which is reflected once more in Figure 11 where the periods of the POPs are inserted into a plot of the wavenumber-frequency power spectrum. The POP method has the advantage of yielding spatial patterns and coefficient time series which define a damped oscillatory subsystem of the full data. Moreover, no a priori assumptions about the relation between standing and travelling components of the spectrum have to be made. The wavenumber-frequency analysis defines the standing part as the coherent part of the westward and eastward moving component of the spectrum in order to solve the problem of determining three parameters, (eastward and westward travelling and the standing component) from a system with only two degrees of freedom (sine and cosine Fourier coefficients). This proceeding is potentially misleading, as can be shown e.g. for certain cases of forced, damped, migrating oscillations where a negative travelling wave variance can result (cf. Luksch et al., 1987).

Nevertheless, like the other studies published so far the POP analysis too was faced with the difficulty of detecting more than the most striking normal modes in real atmospheric data by solely looking at single zonal wave numbers. In order to account for this somewhat artificial approach three additional POP analyses were performed for the geopotential height data, where not the Fourier coefficients for single zonal wave numbers but for wave packets were taken as input, namely the coefficients for waves 1 to 4, waves 5 to 9 and waves 1 to 9. In general, the resulting POPs have lower explained variances and mainly, they only confirm the results already obtained. Especially, they show the apparent preference of the atmosphere for the planetary-scale waves in lower latitudes and for the large-scale waves in higher latitudes. Perhaps, this is indicative for the fact that the POP method is a linear technique which is not able to capture the nonlinear interactions between waves in a wave packet.

Acknowledgement.

The data used in this study were taken from the ECMWF/WMO Global Analysis Data Sets 1980-1987 of the European Center in Reading, England, with the permission of the Deutscher Wetterdienst (DWD), F.R.G.

References.

Barbulescu, M, 1990: Atmosphärische Eigenschwingungen in Modell und Beobachtungen. Ergebnisse einer Wellenzahl-Frequenz-Analyse; Ph. D. thesis at Institut für Geophysik und Meteorologie der Universität zu Köln, Kerpenerstr. 13, D-5000 Köln 41, F.R.G.

Gonella, J., 1972: A rotary-component method for analysing meteorological and oceanographic vector time series; Deep-Sea Research, **19**, 833-846.

Hasselmann, K., 1988: PIPs and POPs: The Reduction of Complex Dynamical Systems Using Principal Interaction and Oscillation Patterns; J. Geophys. Res. **93**, D9, 11.015-11.021.

Hayashi, Y., 1977: On the coherence between progressive and retrogressive waves and a partition of space-time power spectra into standing and traveling parts; J. Appl. Meteor., **16**, 368-373.

Hayashi, Y. , 1982: Space-time spectral analysis and its applications to atmospheric waves; J. Meteor. Soc. Japan, **60**, 156-171.

Longuet-Higgins, 1968: The Eigenfunctions of Laplace's Tidal Equations Over a sphere; Philos. Trans. Roy. Soc. London, **A262**, 511-607.

Luksch, U., H.v. Storch and *Y. Hayashi*, 1987: Monte Carlo Experiments with Frequency-Wavenumber Spectra; MPI Report No. 10, Max-Planck-Institut für Meteorologie, Bundesstr. 55, D-2000 Hamburg, Federal Republic of Germany.

Madden, R.A., 1978: Observations of large-scale traveling Rossby waves; Rev. Geophys. Space Phys., **17**, 1935-1949.

Rossby, C.G. et al., 1939: Relations between variations in the intensity of the zonal circulation of the atmosphere and the displacements of the semipermanent centers of action; J. Mar. Res., **2**, 38-55.

Salby, M, 1984: Survey of planetary-scale transient waves: the state of theory and observations; Rev. Geophys. Space Phys., **22**, 209-236.

Storch, H. von, T. Bruns, I. Fischer-Bruns and *K. Hasselmann*, 1988: Principal Oscillation Pattern Analysis of the 30- to 60-Day Oscillation in General Circulation Model Equatorial Troposphere; J. Geophys. Res. **93**, D9, 11.022-11.036.

Storch, H. von, U. Weese and *J.S. Xu*, 1990: Simultaneous Analysis of Space-Time Variability: Principal Oscillation Patterns and Principal Interaction Patterns with Applications to the Southern Oscillation; Z. Meteorol. **40**, 2, 99-103.

Trenberth, K.E. and *J.G. Olson*, 1988: ECMWF global analyses 1979-1986: Circulation statistics and Data Evaluation; NCAR Tech. Note NCAR/TN-300+STR, 94pp.

Wavenumber	Area	Expl.Var.	POP Period	Decay time	Pos. of Maxima	Stand. Dev.
1	TR	23.4 %	- 7.6	6.1	-30,30	5.0
	TR	25.6 %	-18.7	12.2	-40,40	6.0
2	TR	15.0 %	- 6.1	5.0	-40,30	3.5
	NH	36.4 %	-24.3	9.7	60	29.0
3	TR	7.3 %	- 7.5	5.8	-30,30	2.2
4	TR	14.8 %	- 7.2	9.5	-35,30	3.5

Table 1. POPs for the 3 winters (DJF) 84/85 to 86/87 and for wave numbers 1 to 4 , with
-areas: TR (35°S-35°N), SH (85°S-10°S), NH (10°N-85°N),
-explained variance (refers to time and space filtered data),
-period: in days (negative means westward propagation),
-decay time: in days,
-pos. of amplitude maxima: in degree longitude
(parantheses indicate secondary maxima)
-standard deviation of POP coefficient time series.

Wavenumber	Area	Expl.Var.	POP Period	Decay time	Pos. of Maxima	Stand. Dev.
1	TR	25.1 %	- 6.2	10.0	-30,40	4.5
2	TR	9.4 %	- 7.4	4.4	-30,25	2.7
	TR	17.2 %	-11.5	10.1	-20,40	3.3
3	TR	5.9 %	- 7.2	5.7	-25,25	2.2
4	TR	6.2 %	- 7.2	8.0	-25,40	2.6
1	SH	11.6 %	- 6.8	5.4	-65	12.3
2	SH	10.5 %	12.3	7.7	-45,-65	16.5
3	SH	19.1 %	17.3	7.3	-50	19.5
4	SH	9.0 %	5.8	6.4	-60	16.1
	SH	22.0 %	9.3	10.2	-55	27.5

Table 2: As table 1, but for the three summers (JJA) 85 to 87.

a)

Wavenumber	Area	Expl.Var.	POP Period	Decay time	Pos. of Maxima	Stand. Dev.
5	SH	21.0 %	8.6	7.7	-50	21.3
6	SH	27.8 %	4.5	8.3	-50	13.2
7	SH	51.0 %	3.6	12.3	-50	11.7
8	SH	47.0 %	3.5	9.1	-50	6.6
9	SH	36.2 %	3.7	6.3	-50	4.0
5	SH	12.9 %	5.7	6.9	-55,(-40)	9.3
6	SH	29.0 %	6.9	6.9	-45	14.9
7	SH	15.0 %	4.4	5.4	-45,(-60)	6.8
7	SH	12.1 %	6.0	4.9	-40	8.1
8	SH	17.6 %	5.4	5.2	-40,(-60)	4.1
9	SH	14.7 %	5.5	5.3	-40,(-60)	3.4

b)

Wavenumber	Area	Expl.Var.	POP Period	Decay time	Pos. of Maxima	Stand. Dev.
5	NH	26.3 %	9.4	7.6	50	18.5
6	NH	16.3 %	6.3	5.4	50	11.6
7	NH	22.7 %	4.9	7.0	45	10.3
8	NH	48.9 %	4.3	7.0	42	8.1
9	NH	50.4 %	3.8	6.4	40	6.5
7	NH	20.4 %	6.5	4.8	35, (60)	8.5
7	NH	14.7 %	5.1	4.4	40, 55	9.0
8	NH	14.6 %	4.6	3.8	50, 35	4.5
9	NH	19.7 %	5.0	3.8	50, (30)	4.2

Table 3. As table 1, but for the three winters (DJF) 84/85 to 86/87 and for the zonal wave numbers 5 to 9.

a)

Wavenumber	Area	Expl.Var.	POP Period	Decay time	Pos. of Maxima	Stand. Dev.
5	SH	22.3 %	5.8	6.7	-50	20.3
6	SH	26.0 %	4.2	7.0	-50	11.3
7	SH	19.6 %	4.1	6.7	-50	7.4
8	SH	18.2 %	3.8	5.7	-50	5.3
9	SH	30.3 %	3.9	6.2	-50	4.5
5	SH	6.7 %	4.8	6.3	-55	10.6
6	SH	4.5 %	4.9	4.0	-45,(-60)	8.4
7	SH	9.9 %	4.7	5.0	-40,(-60)	6.2
8	SH	12.6 %	4.5	4.7	-40, -60	4.3
9	SH	12.3 %	4.5	4.8	-40, -60	2.7

b)

Wavenumber	Area	Expl.Var.	POP Period	Decay time	Pos. of Maxima	Stand. Dev.
5	NH	12.3 %	10.4	7.5	60	10.7
6	NH	12.0 %	8.4	6.5	50	7.6
7	NH	25.1 %	8.5	9.0	50	8.7
9	NH	42.3 %	5.0	7.1	50	5.0
6	NH	15.6 %	7.5	6.4	60, (40)	8.3
7	NH	9.6 %	6.5	6.8	50, (65)	5.5

Table 4. As table 1, but for the three summers (JJA) 85 to 87 and for the zonal wave numbers 5 to 9.

Wavenumber	5	6	7	8	9	
Area	SH	SH	SH	SH	SH	
POP period	8.6	4.5	3.6	3.5	3.7	
POP phase speed	6.9	11.0	11.8	10.6	8.9	
Rossby phase speed	10.9	13.9	15.8	16.9	17.7	
Wavenumber	5	6	7	7	8	9
Area	SH	SH	SH	SH	SH	SH
POP period	5.7	6.9	4.4	6.0	5.4	5.5
POP phase speed	8.1	7.9	10.6	8.4	7.6	7.1
Rossby phase speed	6.7	10.9	13.3	7.9	14.9	11.2
Wavenumber	5	6	7	8	9	
Area	NH	NH	NH	NH	NH	
POP period	9.4	6.3	4.9	4.3	3.8	
POP phase speed	5.6	7.9	9.5	10.3	10.4	
Rossby phase speed	1.1	4.2	8.3	11.7	13.0	
Wavenumber	7	7	8	9		
Area	NH	NH	NH	NH		
POP period	6.5	5.1	4.6	5.0		
POP phase speed	8.3	7.4	8.1	6.6		
Rossby phase speed	8.6	4.5	7.2	8.1		

Table 5. Comparison for DJF of phase speeds (unit m/s) as derived from the POP period and as computed from the Rossby formula (1) for zonal wave numbers 5 to 9. The values are given for the latitudes with maximum wave amplitudes. The mean zonal wind U is computed from the ECMWF wind data with typical values of U=20.8 m/s at 50°S and U=11.1 m/s at 50°N.

Figure Captions.

Figure 1. Different representation of POPs $P^1 + iP^2$ corresponding to
a) a purely zonally propagating wave,
b) a standing wave,
c) a meandering wave with zonal and meridional propagation.
The transformation is given through the cycle
$$\ldots \longrightarrow P^2 \longrightarrow P^1 \longrightarrow -P^2 \longrightarrow -P^1 \longrightarrow P^2 \longrightarrow \ldots \quad .$$
The uppper two rows show the representation as real and imaginary patterns P^1 and P^2. The bottom two rows show the representation as amplitude/phase diagram with amplitudes and phases of the zonal wave plotted against latitude (real part: light, imaginary part: heavy curve) (cf. Storch et al., 1988: Fig. 2).

Figure 2. POP 1 for TR-analysis of wave number 1 of geopotential height at 500 hPa for winters (DJF) 84/85 to 86/87 (Oscillation period: 7.6 days westwards).
a) Representation as 2-d plots.
b) Representation in amplitude and phase diagrams.

Figure 3. Variance spectra, phase spectrum and squared coherence of cross spectral analysis between real and imaginary part of the POP coefficient time series for the POP in Figure 2.

Figure 4. Associated correlation patterns for the POP in Figure 2 for geopotential height data with wave 1-4 remained and annual, semi-annual cycle and mean removed.
a) Associated pattern for level 850 hPa (real and imaginary part in gpm, variance in % explained by the pattern)
b) Plot of phases and amplitudes of associated patterns for the levels 850, 700, 500, 300, 200, 100 hPa (to have unique phases the associated patterns for the data only with wave number 1 retained are used).

Figure 5. POP 1 for TR-analysis of wave numbers 2-4 of geopotential height at 500 hPa for winters (DJF) 84/85 to 86/87.
a) Wave number 2: oscillation period 6.1 days westwards.

b) Wave number 3: oscillation period 7.5 days westwards.
c) Wave number 4: oscillation period 7.2 days westwards.

Figure 6. POP 1 for NH-analysis of wave number 2 of geopotential height in in 500 hPa for winters (DJF) 84/85 to 86/87 (Oscillation period: 24.3 days westwards).

Figure 7. Wavenumber-frequency analysis for zonal wave number 1 of geopotential height at 300 hPa, derived from 8 winters (DJF,79/80 through 86/87) of twice daily ECMWF analyses. From Barbelescu, 1990.
a) Squared coherence relative to reference latitude 39°N .
b) Phase difference relative to 60°N for the period of 5 days westwards (unit: ° longitude).

Figure 8. POP 1 for SH-analysis of wave number 6 of geopotential height at 500 hPa for winters (DJF) 84/85 to 86/87 (Oscillation period: 3.5 days eastwards).
a) Real and imaginary parts of POP.
b) Variance spectra and squared coherence spectrum of the real and the imaginary part of the POP coefficient time series.

Figure 9. POP 1 for NH-analysis of wave number 6 of geopotential height at 500 hPa for winters (DJF) 84/85 to 86/87 (Oscillation period: 4.3 days eastwards).

Figure 10. Associated correlation patterns for the POPs in figures 8, 9 for geopotential height data at 850 hPa with wave 5-9 remained and annual, semi-annual cycle and mean removed (real and imaginary part in gpm, variance in % explained by the patterns).
a) Southern hemisphere POP.
b) Northern hemisphere POP.

Figure 11. Wavenumber-frequency power spectrum (travelling part, unit $gpm^2/\Delta f$) of geopotential at 50°S in the 500 hPa level, averaged over 3 winters (DJF) 84/85 to 86/87, together with the frequencies ($days^{-1}$) and phase speeds (ms^{-1}) of the POPs for each wave number (crosses).

Figure 1

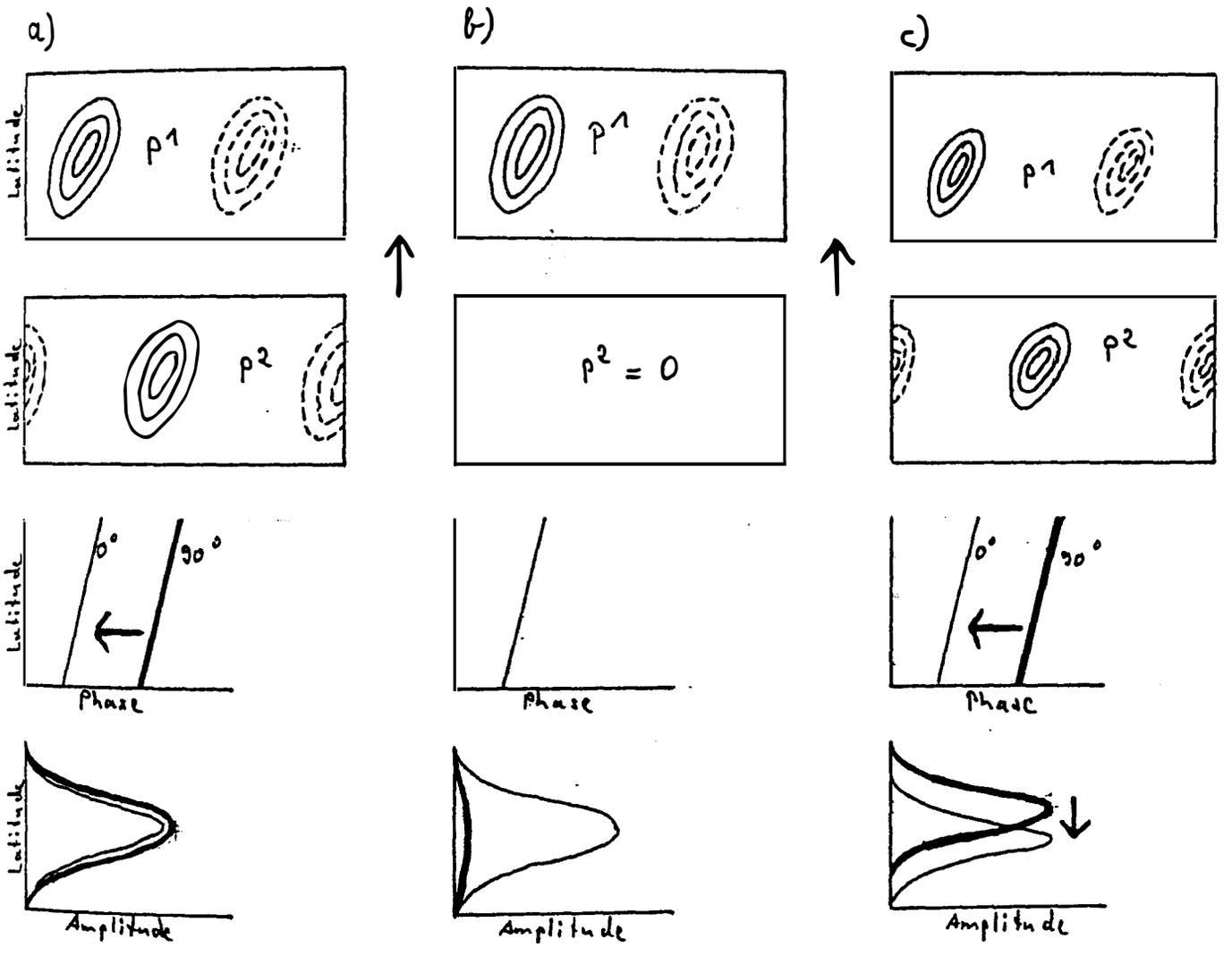

Figure 1. Different representation of POPs $\mathbf{P}^1 + i\mathbf{P}^2$ corresponding to

a) a purely zonally propagating wave,

b) a standing wave,

c) a meandering wave with zonal and meridional propagation.

The transformation is given through the cycle

$$\ldots \longrightarrow \mathbf{P}^2 \longrightarrow \mathbf{P}^1 \longrightarrow -\mathbf{P}^2 \longrightarrow -\mathbf{P}^1 \longrightarrow \mathbf{P}^2 \longrightarrow \ldots \quad .$$

The uppper two rows show the representation as real and imaginary patterns $\mathbf{P}^1$ and $\mathbf{P}^2$. The bottom two rows show the representation as amplitude/phase diagram with amplitudes and phases of the zonal wave plotted against latitude (real part: light, imaginary part: heavy curve) (cf. Storch et al., 1988: Fig. 2).

Figure 2

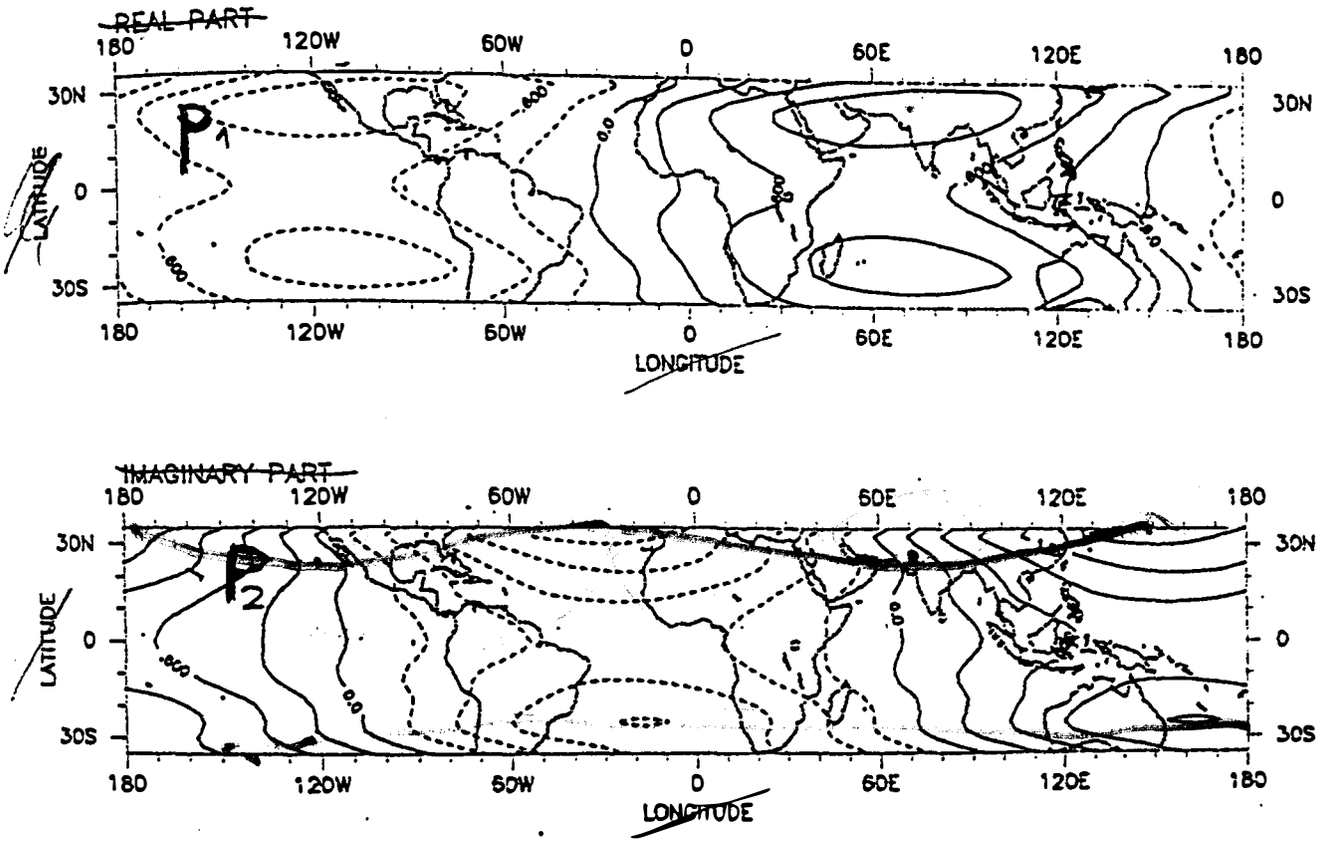

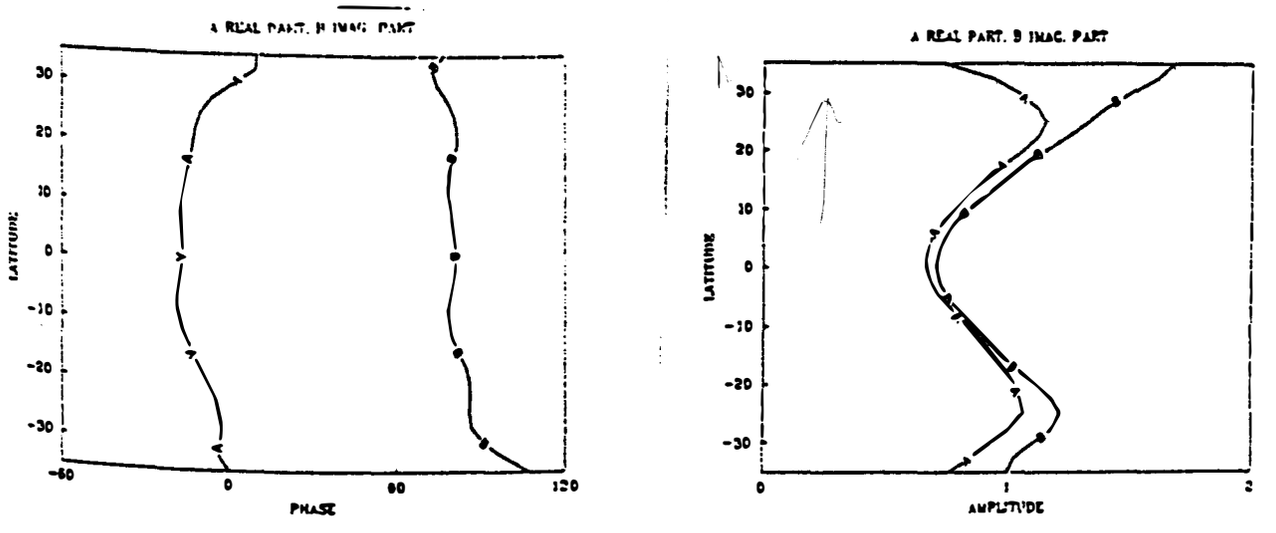

Figure 2. POP 1 for TR-analysis of wave number 1 of geopotential height at 500 hPa for winters (DJF) 84/85 to 86/87 (Oscillation period: 7.6 days westwards).

a) Representation as 2-d plots.

b) Representation in amplitude and phase diagrams.

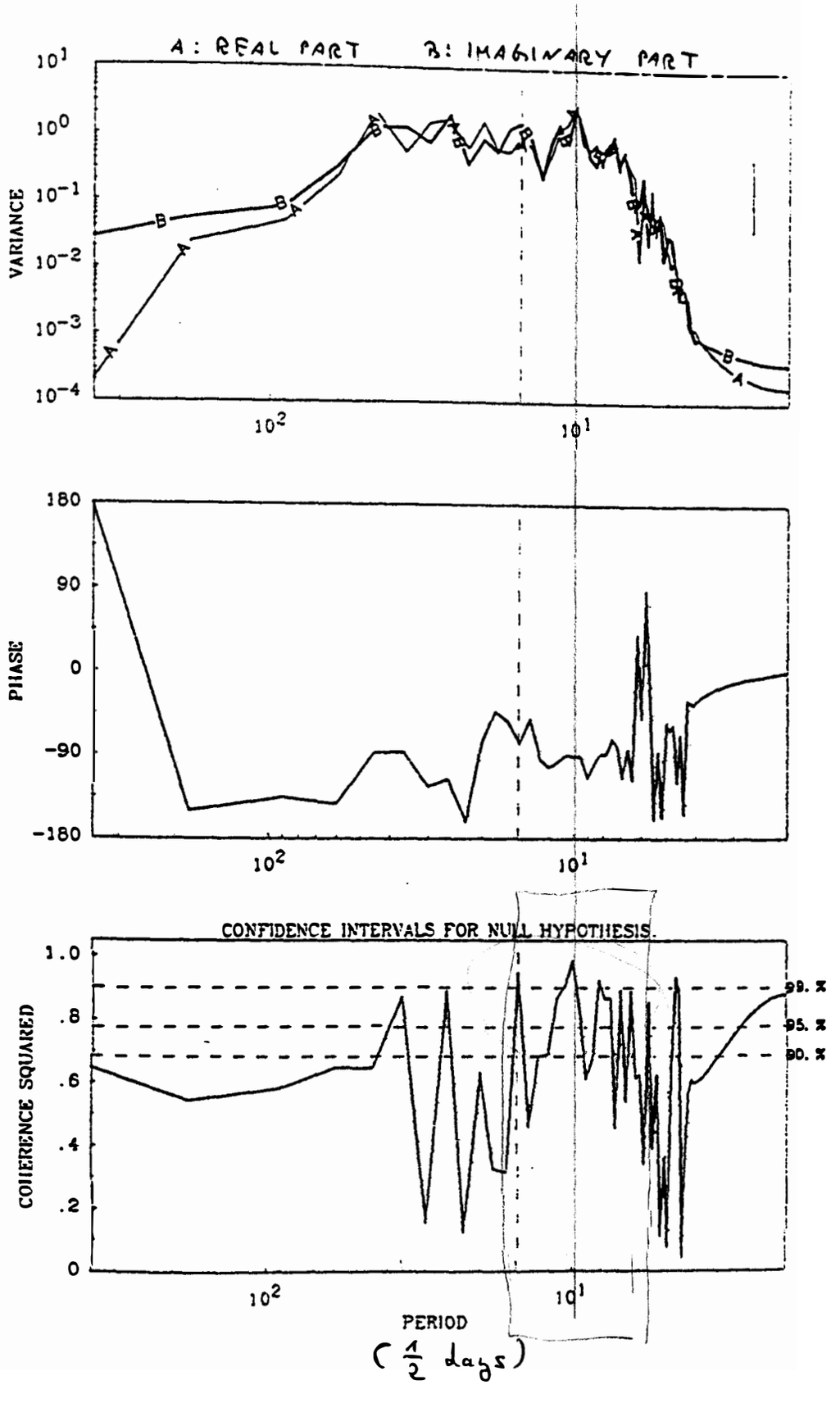

Figure 3. Variance spectra, phase spectrum and squared coherence of cross spectral analysis between real and imaginary part of the POP coefficient time series for the POP in Figure 2.

Figure 4

REAL PART

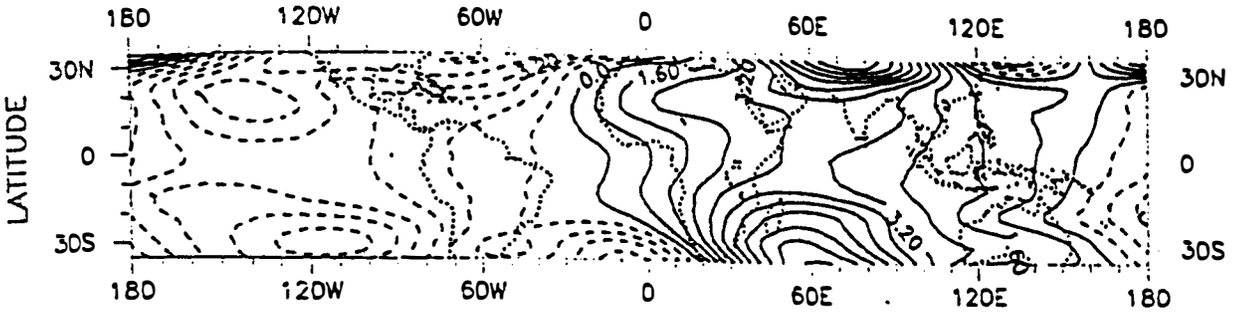

IMAGINARY PART

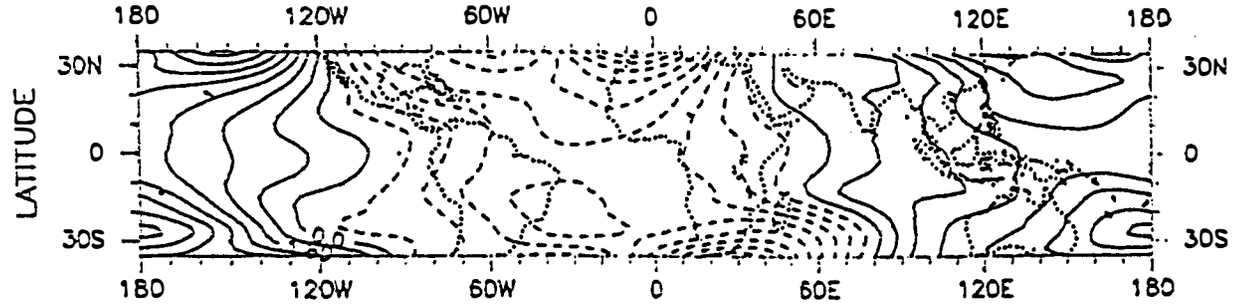

EXPLAINED VARIANCE

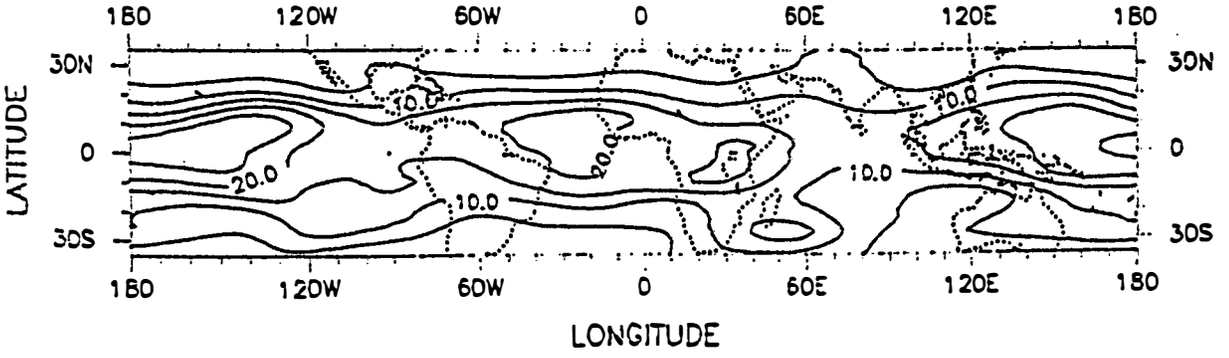

4)

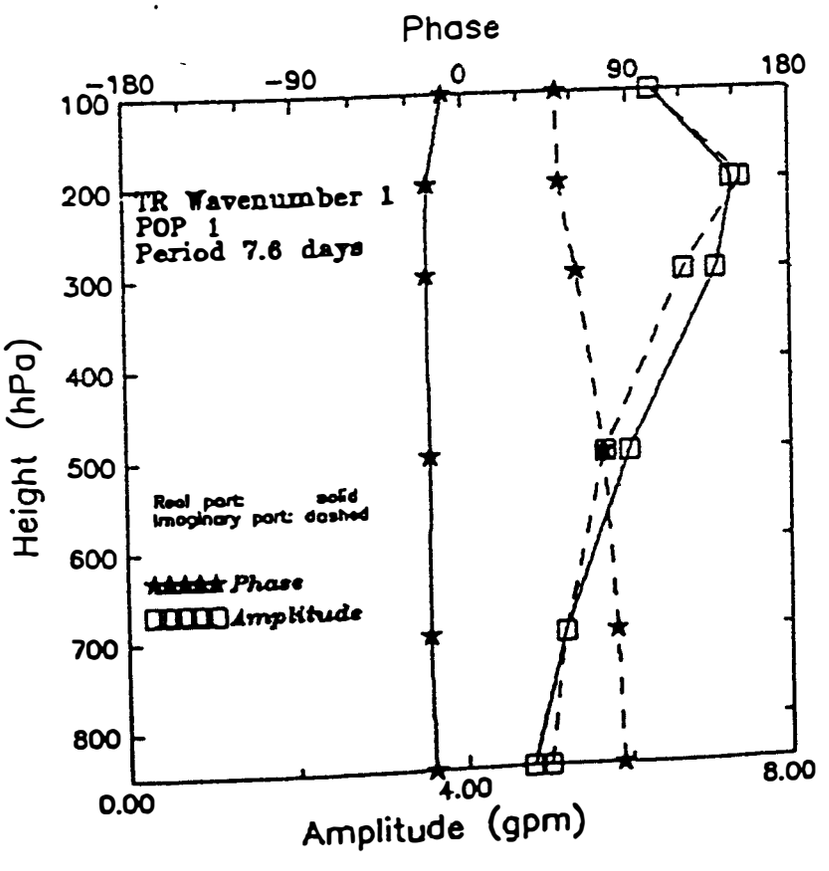

Figure 5

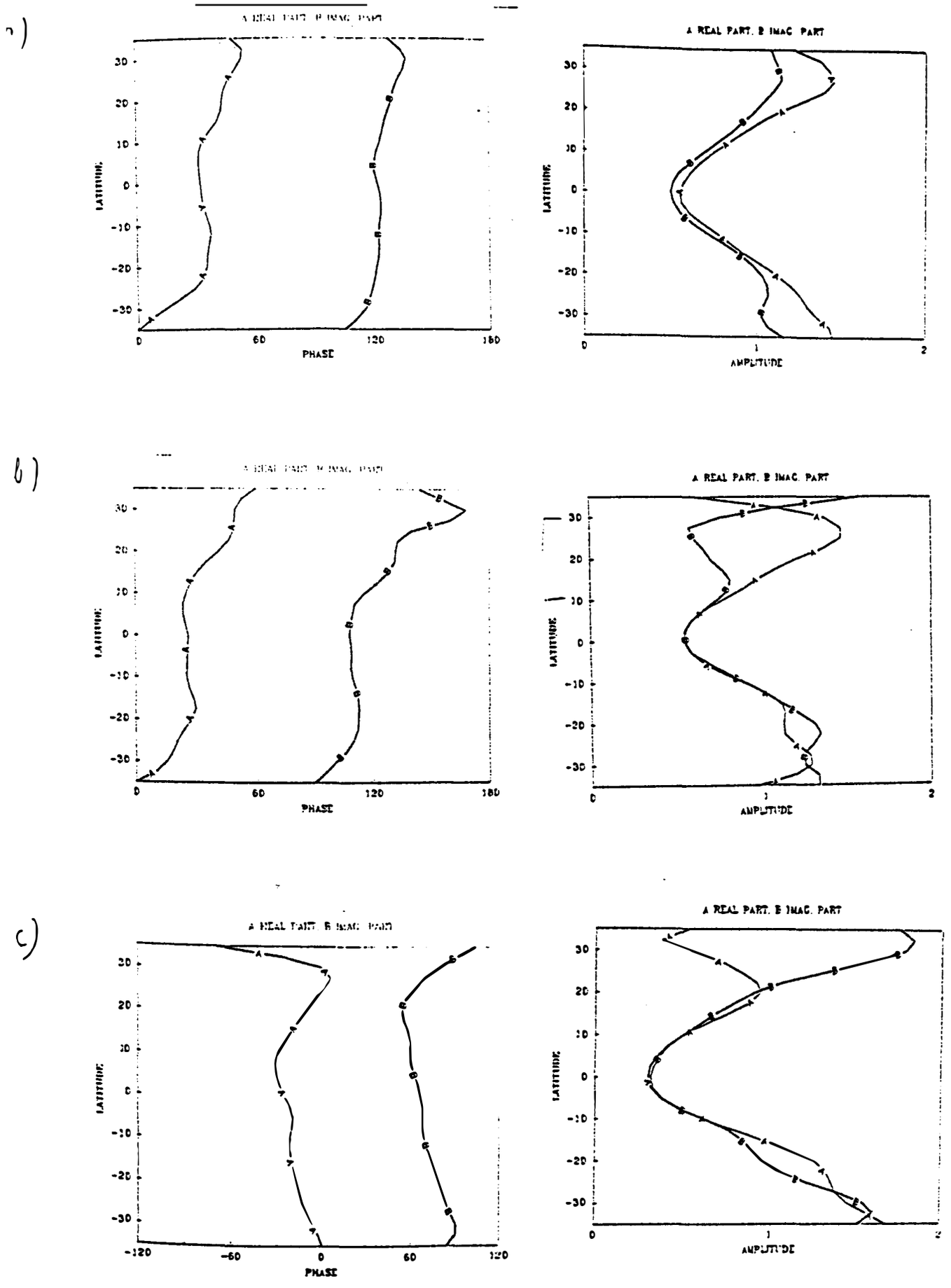

Figure 5. POP 1 for TR-analysis of wave numbers 2-4 of geopotential height at 500 hPa for winters (DJF) 84/85 to 86/87.

a) Wave number 2: oscillation period 6.1 days westwards.

b) Wave number 3: oscillation period 7.5 days westwards.

c) Wave number 4: oscillation period 7.2 days westwards.

Figure # 6

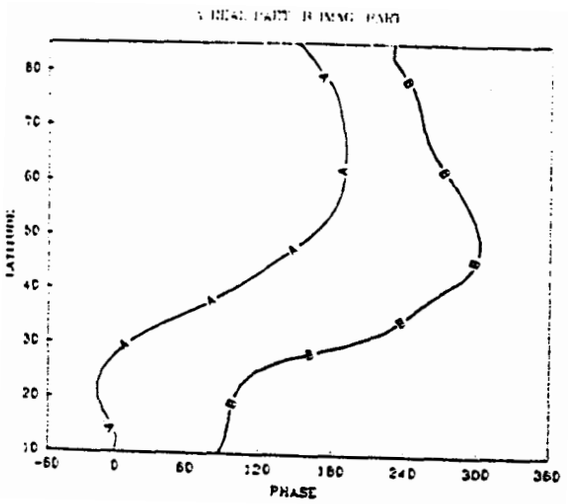

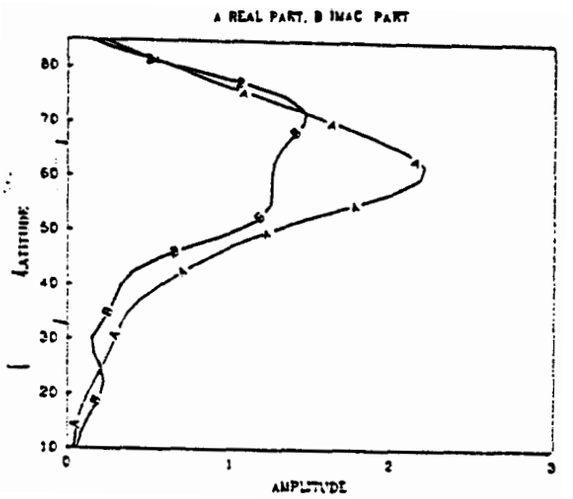

A: real part, B: imaginary part

Figure 6. POP 1 for NH-analysis of wave number 2 of geopotential height in in 500 hPa for winters (DJF) 84/85 to 86/87 (Oscillation period: 24.3 days westwards).

Figure 7

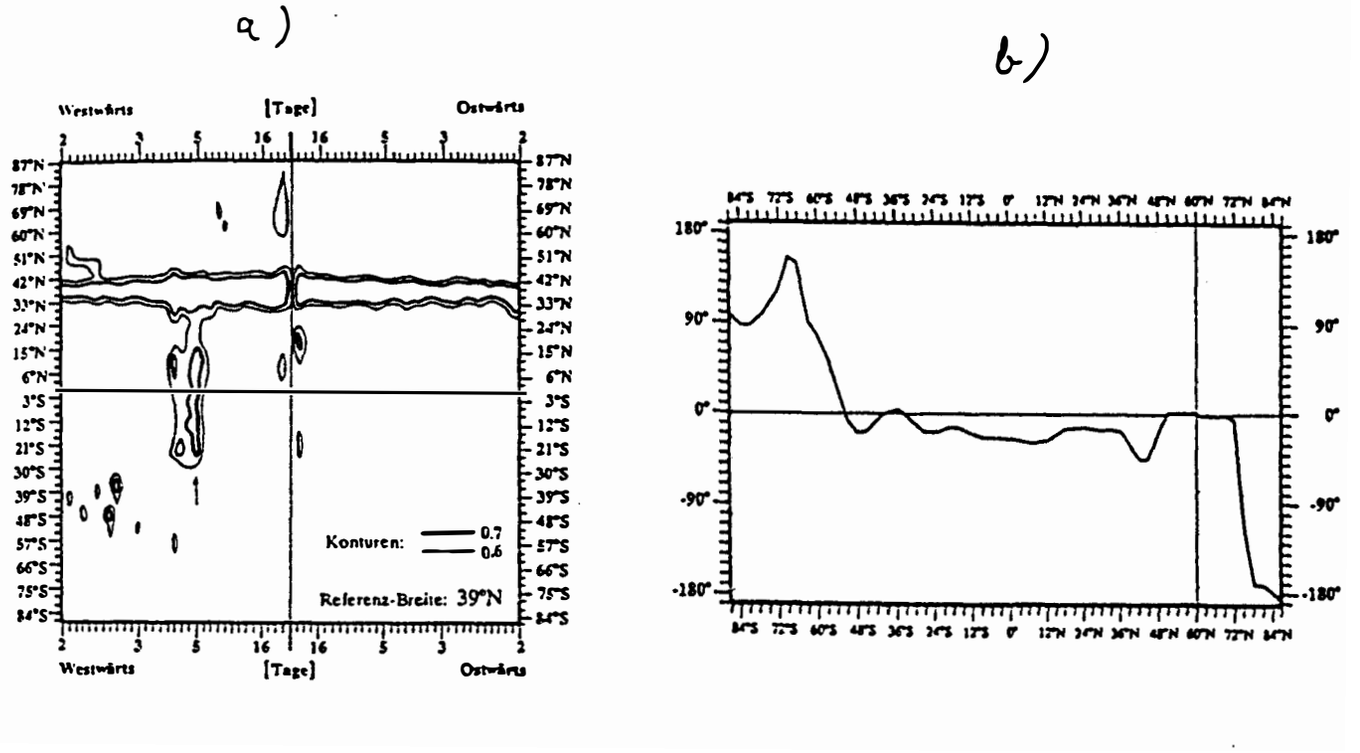

Figure 7. Wavenumber-frequency analysis for zonal wave number 1 of geopotential height at 300 hPa, derived from 8 winters (DJF,79/80 through 86/87) of twice daily ECMWF analyses. From Barbelescu, 1990.

a) Squared coherence relative to reference latitude 39°N .

b) Phase difference relative to 60°N for the period of 5 days westwards (unit: ° longitude).

Figure 8

a)

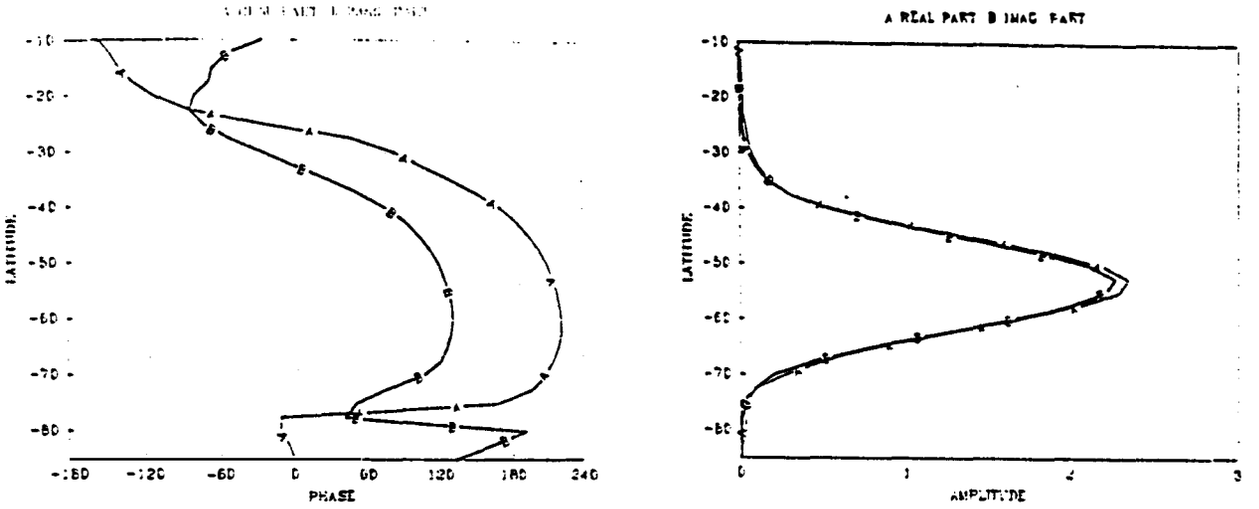

A : real part , B : imaginary part

b)

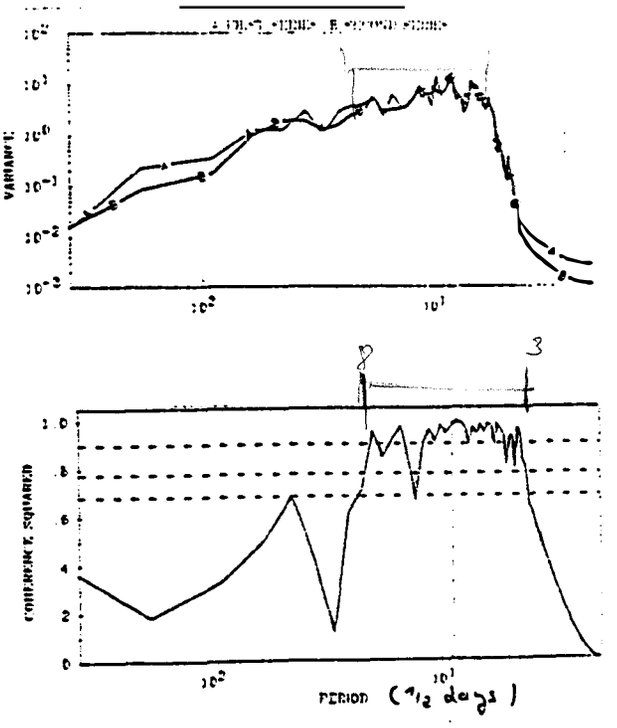

Figure 8. POP 1 for SH-analysis of wave number 6 of geopotential height at 500 hPa for winters (DJF) 84/85 to 86/87 (Oscillation period: 3.5/4 days eastwards).

a) Real and imaginary parts of POP.

b) Variance spectra and squared coherence spectrum of the real and the imaginary part of the POP coefficient time series.

Figure 9

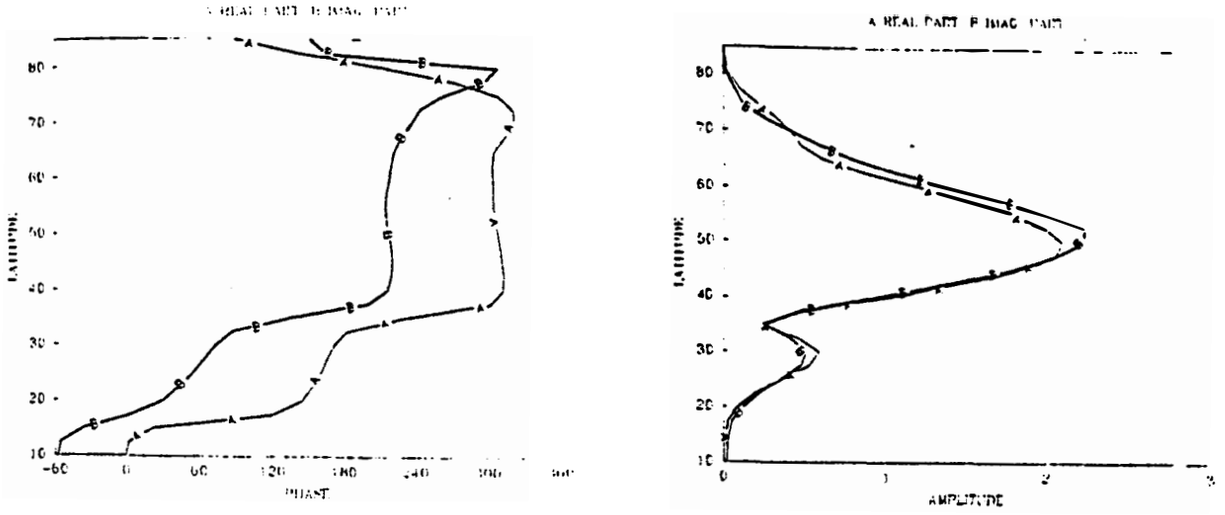

A: real part, B: imaginary part

Figure 9. POP 1 for NH-analysis of wave number 6 of geopotential height at 500 hPa for winters (DJF) 84/85 to 86/87 (Oscillation period: 4.3 days eastwards).

Figure 10

a)

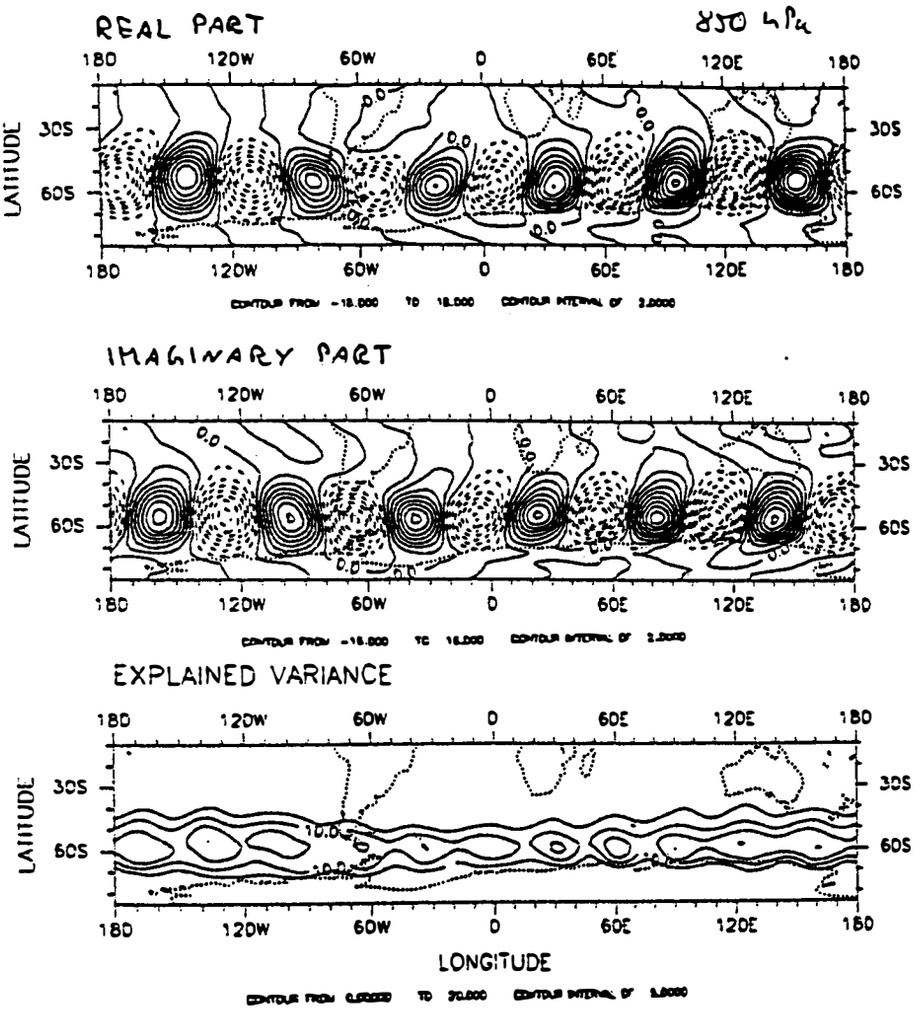
REAL PART
850 hPa
180 120W 60W 0 60E 120E 180
LATITUDE
30S
60S
IMAGINARY PART
EXPLAINED VARIANCE
LONGITUDE

b)

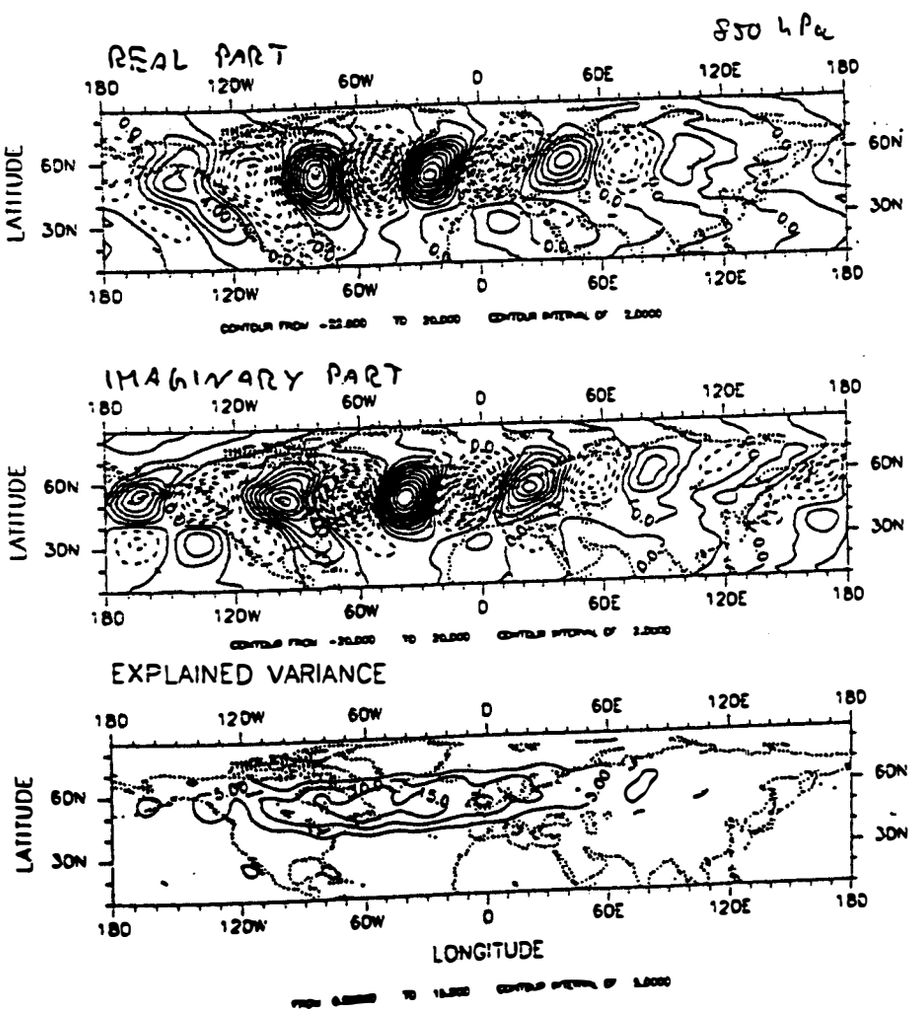
850 hPa
REAL PART
180 120W 60W 0 60E 120E 180
LATITUDE
60N
30N
IMAGINARY PART
EXPLAINED VARIANCE
LONGITUDE

Figure 11

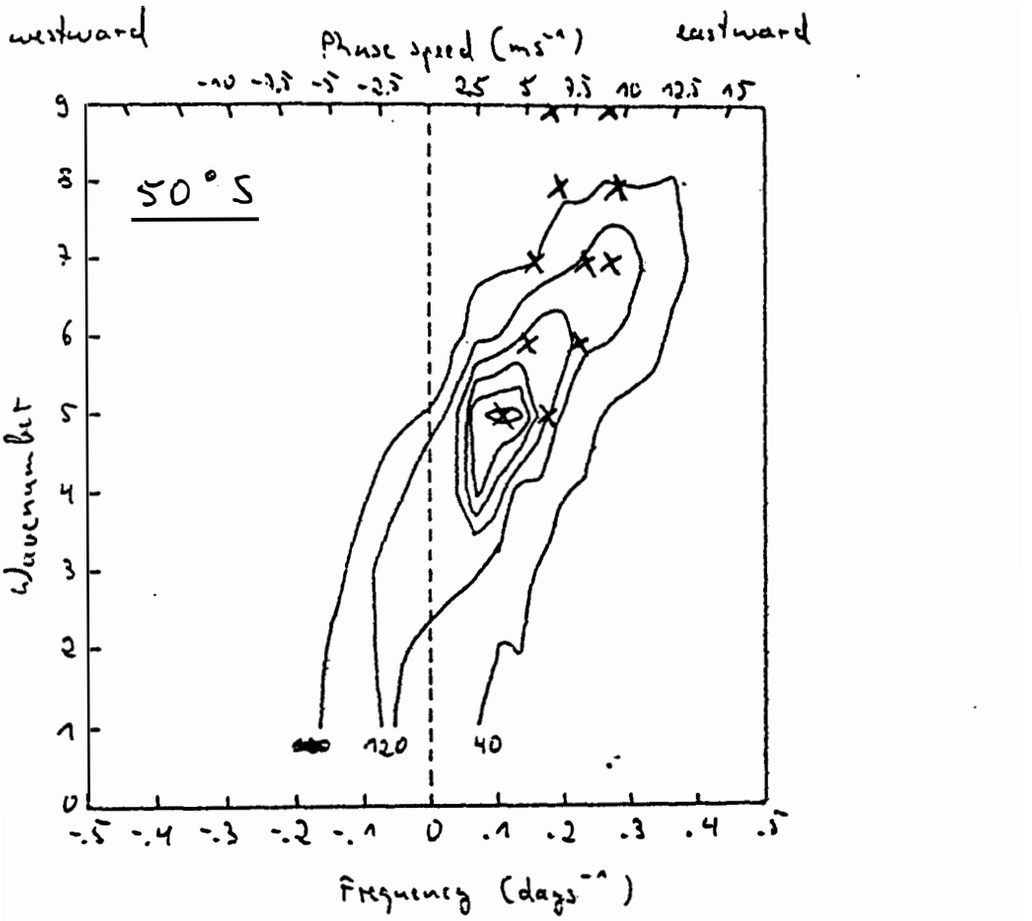

Figure 11. Wavenumber-frequency power spectrum (travelling part, unit $gpm^2/\Delta f$) of geopotential at 50°S in the 500 hPa level, averaged over 3 winters (DJF) 84/85 to 86/87, together with the frequencies ($days^{-1}$) and phase speeds (ms^{-1}) of the POPs for each wave number (crosses).